Competing orders and spin-density-wave instability in La(O$_{1-x}$F$_x$)FeAs

J. Dong, H. J. Zhang, G. Xu, Z. Li, G. Li, W. Z. Hu, D. Wu, G. F. Chen, X. Dai,
J. L. Luo, Z. Fang[a] and N. L. Wang[b]

Beijing National Laboratory for Condensed Matter Physics, and Institute of Physics,
Chinese Academy of Sciences - Beijing 100190, China

Abstract – The interplay between different ordered phases, such as superconducting, charge or spin ordered phases, is of central interest in condensed-matter physics. The very recent discovery of superconductivity with a remarkable $T_c = 26$ K in Fe-based oxypnictide La(O$_{1-x}$F$_x$)FeAs (see Kamihara Y. *et al., J. Am. Chem. Soc.*, **130** (2008) 3296) is a surprise to the scientific community and has generated tremendous interest. The pure LaOFeAs itself is not superconducting but shows an anomaly near 150 K in both resistivity and dc magnetic susceptibility. Here we provide combined experimental and theoretical evidences showing that a spin-density-wave (SDW) state develops at low temperature, in association with electron Nematic order. The electron-doping by F suppresses the SDW instability and induces the superconductivity. Therefore, the La(O$_{1-x}$F$_x$)FeAs offers an exciting new system showing competing orders in layered compounds.

Both charge-density wave (CDW) and spin-density-wave instabilities may develop in the presence of Fermi surface (FS) nesting [1], as shown in many transition metal compounds, such as 2H-NbSe$_2$ [2] and Cr [3]. The difference is that CDW couples to lattice and SDW couples to spin. The CDW or SDW instabilities may compete with other possible orderings, and complicated phase diagrams are often drawn due to their interplay. This is exactly what happens for LaOFeAs as shown in this paper. LaOFeAs crystalizes in layered square lattice with Fe layers sandwiched by two As layers (up and down), each Fe is coordinated by As tetrahedron [4]. Its electronic properties are dominated by the (FeAs)-triple-layers, which contribute mostly to the electronic state around the Fermi level (E_f). The electronic structure of LaOFeAs is quasi–two-dimensional and very similar to typical semi-metal, namely there are hole-like FS cylinders around the Γ-Z line of the Brillouin zone (BZ), and electron-like FS cylinders around the M-A line of the BZ (except a small 3D FS around the Z-point of BZ) [5–9]. We will show here that surprisingly strong FS nesting exists by connecting the hole and electron

FS by a commensurate vector $q = (\pi, \pi, 0)$. This leads to SDW instability, and it is the main cause of the anomaly observed near 150 K experimentally. The spontaneously symmetry-broken SDW state is characterized in terms of reduced carrier density due to (partial) FS nesting, enhanced conductivity due to the reduction of scattering channel, and loss of 4-fold rotational symmetry with negligible change of lattice.

Series of La(O$_{1-x}$F$_x$)FeAs samples are fabricated by the solid-state reaction using Fe$_2$O$_3$, Fe, La, As, and LaF$_3$ as starting materials. LaAs was obtained by reacting La chips and As pieces at 500 °C for 15 hours and then at 850 °C for 2 hours. The raw materials were thoroughly mixed and pressed into pellets. The pellets were wrapped with Ta foil and sealed in an evacuated quartz tube under argon atmosphere. They were then annealed at 1150 °C for 50 hours. The phase purity was checked by a powder X-ray diffraction method using Cu $K\alpha$ radiation at room temperature. The XRD patterns are well indexed on the basis of tetragonal ZrCuSiAs-type structure with the space group $P4/nmm$. The electrical resistivity was measured by a standard 4-probe method. The specific heat measurement was carried out using a thermal relaxation calorimeter. The heat capacity of addenda was carefully calibrated before measurement.
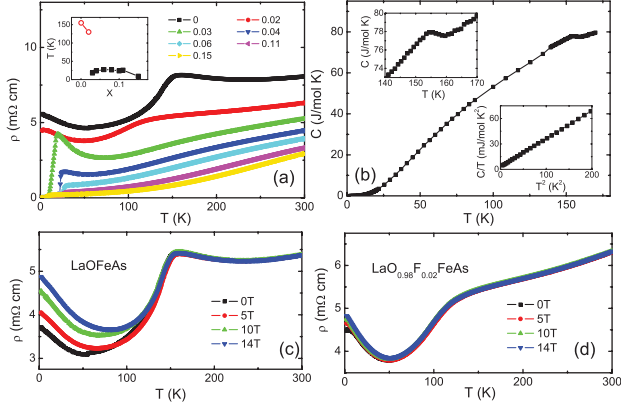
Fig. 1: (Color online) (a) The electrical resistivity *vs.* temperature for a series of LaO$_{1-x}$F$_x$FeAs. Inset: The phase diagram showing the anomaly (red circle) and superconducting transition (black square) temperatures as a function of F content. (b) Specific heat *vs.* temperature curve. Upper inset: the expanded region near the transition temperature; lower inset: a plot of C/T *vs.* T^2. (c) and (d) T-dependent resistivity under magnetic field for the pure and 2% F-doping samples, respectively.

All these measurements were performed down to 1.8 K in a Physical Property Measurement System (PPMS) of Quantum Design company. Optical reflectance measurement were performed on Bruker 113v and 66v/s spectrometers in the frequency range from 20 cm^{-1} to 15000 cm^{-1} at different temperatures. The samples were polished and shinny and metallic bright surface was obtained. An *in-situ* gold overcoating technique was used for the experiment. Optical conductivity was derived from Kramers-Kronig transformation of reflectance. The first-principles calculations were done using the plane-wave pesudopotential method and the generalized gradient approximation (GGA) for the exchange-correlation potential. For the 1×1 unit cell, the calculated results are identical to those performed by other people [6,7].

Figure 1(a) shows the temperature dependence of the resistivity. The pure LaOFeAs sample has rather high dc resistivity value and very weak temperature dependence at high temperature, but below roughly 150 K, the resistivity drops steeply, with an upturn at lower temperature (below 50 K). At 2% F-doping, the overall resistivity decreases and the 150 K anomaly shifts to the lower temperature and becomes less pronounced. At 3% F-doping, the anomaly could not be seen, and a superconducting transition occurs at $T_c = 17$ K. With further increasing F content, and the superconducting transition temperature increases with the highest $T_c = 28$ K seen at 6–8% F-doping. A T_c *vs.* F-content phse diagram is plotted in the inset of fig. 1(a).

Apparently, superconductivity competes with the phase showing the anomaly in this system. To identify whether the anomaly near 150 K in LaOFeAs is due to a phase transition, we performed the specific heat measurement. Figure 1(b) shows the specific-heat data as a function of temperature. A very clear specific-heat jump is seen at a temperature close to 155 K (see the expanded plot in the upper inset). A good linear T^2-dependence indicates that the specific heat C is mainly contributed by electrons and phonons. The fit yields the electronic coefficient $\gamma = 3.7$ mJ/mol $\cdot$ K^2 and the Debye temperature $\theta_D = 282$ K. Note that the electronic coefficient γ is significantly smaller than the values obtained from the band structure calculations being about 5.5–6.5 mJ/mol $\cdot$ K^2 [6,7]. This result is unconventional, because usually the band structure calculation gives a value smaller than the experimental data, their difference is ascribed to the renormalization effect. We recently measured a Ni-based oxypnictide La(O$_{0.9}$F$_{0.1}$)NiAs, and indeed found that the experimental electronic coefficient is larger than the band structure calculation [10]. As we shall show below that a partial energy gap formation is revealed at low temperature and explained as originated from the SDW instability, the smaller experimental value here could be naturally accounted for by the gap formation which removes parts of the density of states below the phase transition.

We also measured the resistivity under magnetic field. Figures 1(c) and (d) show the results for the pure and 2% F-doping samples, respectively. The anomaly transition temperature is rather insensitive to magnetic field up to 14 T, however sizable positive magnetoresistance are observed at low temperature for pure LaOFeAs. The positive magnetoresistance could be understood in terms of the suppression of SDW order (and therefore enhanced spin scattering) by external magnetic field. After 2% F-doping, the low temperature magnetoresistance becomes much weaker, which suggests the same tendency that F-doping tries to suppress the anomaly around 150 K. The overall picture is pretty much similar to the elemental Cr, a typical SDW system, where transition temperature is extremely insensitive to magnetic field and sizable magnetoresistance exists after SDW transition [3].

Important information about the nature of the phase transition could be obtained from the optical measurement. Figure 2(a) shows the temperature-dependence of the reflectance in the far-infrared region for the pure LaOFeAs sample. The reflectance at 300 K over a broad frequency range is shown in the upper inset. Even though the measurement was performed on polycrystalline samples, two important experimental findings regarding the phase transition could be unambiguously drawn from the measurement. First, at low temperature, the reflectance is strongly suppressed below the frequency of 400 cm^{-1}. This is dramatically different from the F-doped LaO$_{0.9}$F$_{0.1-\delta}$FeAs superconducting sample where a monotonous increase of the reflectance was seen [11]. The suppression is a strong indication for the formation of an energy gap in the density of state. Note that the reflectance at very low frequency increases fast and exceeds the values at high temperature, *e.g.* above the phase transition. This indicates that the compound is still metallic even below the phase transition, being consistent with the dc resistivity measurement which reveals an
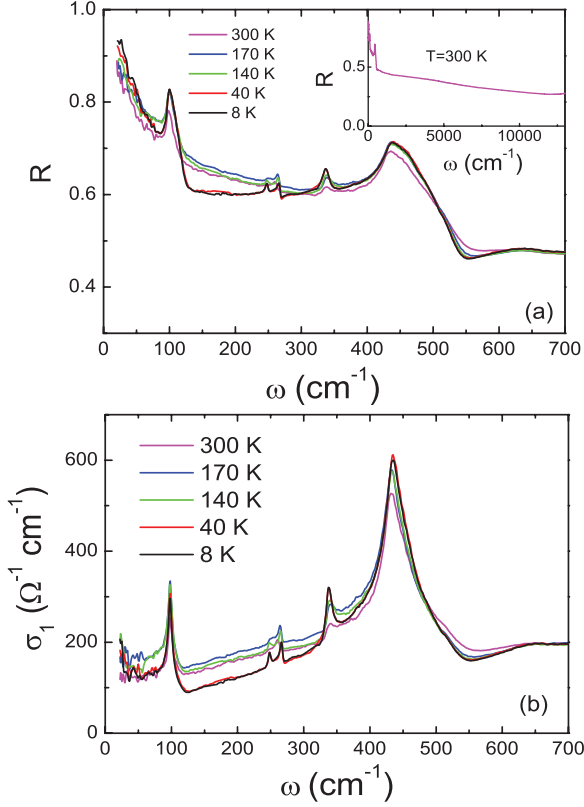
Fig. 2: (Color online) (a) The reflectance spectra in the far-infrared region at different temperatures for the pure LaOFeAs sample. The inset shows the reflectance over a broad frequency range at room temperature. (b) The conductivity spectra at different temperatures.
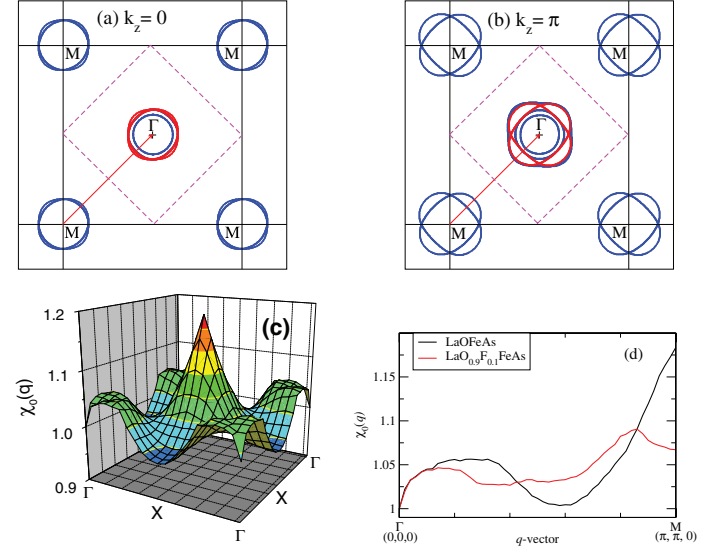

Fig. 3: (Color online) (a) and (b) are the Fermi surfaces (FS) cut at the $k_z = 0$ and π planes, respectively. The blue lines are original calculated FS, while red lines indicate the FS shifted by $q = (\pi, \pi, 0)$. Significant nesting is clear. (c) The calculated Lindhard response functionn $\chi_0(q)$. It is strongly peaked at the M-point. (d) The $\chi_0(q)$ along the Γ-M line. The peak at the M-point is much suppressed by F-doping.

enhanced conductivity. The data indicate clearly that only partial or some of the Fermi surfaces are gapped. We note that the gap is very small, roughly in the range of 150–350 cm^{-1}. Below 50 cm^{-1}, we find a sharp upturn for conductivity spectrum at 8 K (see fig. 2(b)), suggesting development of very narrow Drude compound, which should be linked to the survived FS in the SDW state.

Second, a number of pronounced phonon structures are seen in the reflectance and conductivity spectra. Note that infrared spectroscopy probes phonon modes only near Γ-point, the frequencies of the observed infrared active modes are basically in agreement with the calculations by Singh and Du [6]. Upon cooling the sample below the transition temperature, no splitting or new phonon mode is observed[1]. Considering the polycrystalline nature of the sample which has random orientations of the ab-plane and the c-axis, the absence of new or splitting of phonon mode suggests that there is negligible lattice distortion across the phase transition. Therefore, the phase transition is not likely to be driven by CDW instability.

In the following we shall illustrate that the transition is caused by the SDW transition due to the Fermi surface nesting from first-principles calculations. As we will show below, after the SDW transition, a stripe like spin ordering pattern appears which breaks the 4-fold rotational symmetry and induces a nematic oder in the charge sector.

Using the experimental high-temperature structure ($P4/nmm$ symmetry), our calculated electronic structures and Fermi surfaces are identical to those done by other people [5–7]. By cutting the BZ into fixed-k_z planes, circle like FS are resolved (as shown in fig. 3(a) and (b) for $k_z = 0$ and $k_z = \pi$ planes, respectively). Surprisingly, by shifting the circles around the M-points to the Γ-point, *i.e.* by a vector $q = (\pi, \pi, 0)$, the electron-like FS will largely overlap with the hole-like FS, suggesting significant nesting effect. For example, for the $k_z = 0$ plane, the small electron circle almost exactly overlaps with the large hole circle after shifting by q. Similar thing happens for the $k_z = \pi$ plane. The nesting effect can be quantitatively estimated by calculating the Lindhard response function as shown in fig. 3(c) and (d). The calculated $\chi_0(q)$ is strongly peaked at the M-point for undoped compound, and it is much suppress by electron-doping, because the up-shift of the Fermi level tends to reduce the size of hole-like FS and enlarge the electron FS. The existence of strong nesting effect would suggest that certain kinds of ordering, either CDW or SDW, may develop at low temperature. As mentioned above, the absence of any splitting or new phonon mode after the transition suggests that the structural distortion, if any, is negligible, the

---

[1]A phonon mode at 247 cm^{-1} is very week at high temperature but eminently enhanced at low temperture. We have carefully checked two different samples, and concluded that mode exists both below and above the phase transition.
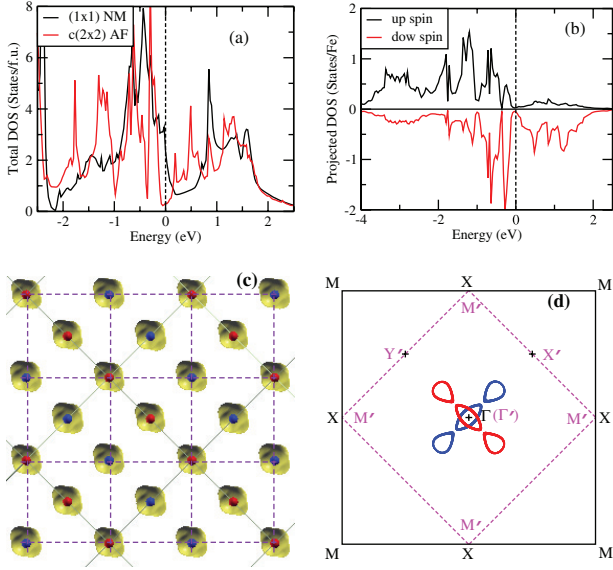
Fig. 4: (Color online) (a) The total DOS of (1×1) NM and $(\sqrt{2} \times \sqrt{2})$ AF solutions. The reduction of $N(E_F)$ is about 7. (b) The projected DOS of Fe site for the AF solution. (c) The stripe-like ordering pattern of the Fe plane and the charge distribution (occupied). The Fe atoms are indicated by red and blue spheres with up and down spin, respectively. The original (1×1) unit cell is indicated by the dashed lines. (d) The calculated FS of the AF state. The BZ special points of the $(\sqrt{2} \times \sqrt{2})$ cell are indicated by symbols with prime. The red lines are rotated from blue lines, corresponding to the 90 degrees rotation of stripe orientation.

CDW ordering is therefore unlikely. Nevertheless, here we provide further theoretical evidences.

The commensurate nesting vector suggests the doubling of the unit cell to be $(\sqrt{2} \times \sqrt{2})$ (*i.e.* the folding of the BZ along the dashed lines shown in fig. 3(a) and (b)). We have tried to optimized the structure of non-magnetic (NM) state without using any symmetry, the solution always recover to the original (1×1) structure. However, among several possible magnetic solutions, one antiferromagnetic (AF) ordered state (see the ordering pattern shown in fig. 4) can be stabilized with about $40 \, \mathrm{meV/Fe}$ lowering in energy and about $1.5 \, \mu_B/\mathrm{Fe}$ for the spin moment compared to (1×1) NM solution. Clearly the nesting instability likes to couple with spin rather charge. It is important to note that only part of the FS are nested, as the results, the system remains to be metallic and only partial gap opens at E_F. The density of state at E_F is reduced significantly compared with original (1×1) NM solution as shown in fig. 4. All those factors are exactly what were observed in our experiments. Treating the F-doping by virtue crystal approximation, we found that both nesting effect and the stabilization energy of AF solution are suppressed, again explain the experimental observation.

The obtained AF ordered state is different with the (1×1) NM state in the sense that 4-fold rotational symmetry is broken due to the presence of magnetic ordering, and the stripe-like ordering pattern is revealed for the Fe plane (as shown in fig. 4(c)). However, if the stripe orientation is rotated by 90 degrees for the neighboring Fe plane stacking along z, the lattice parameters may remain to be 4-fold invariant. Furthermore, if we concentrate on the charge (rather than magnetic density) distribution, the translational symmetry of total charge remains to be the same as original (1×1) structure (as shown in fig. 4(c). As we mentioned, this is the reason why no new phonon modes are observed. It deserves to remark that, in the ordered state, the charge at Fe site has a preferentially aligned distribution along stripe direction (see fig. 4(c)). The fact that charge density picks up of preferred direction after a spontaneous symmetry-breaking in spin sector could be considered as a formation of nematic order [12]. Here, the order is characterized by a 4-fold rotational symmetry broken.

$* * *$

Additional Remark: After we submitted this paper (arXiv:0803.3426), neutron scattering experiments (arXiv:0804.0795) were reported to confirm our predicted SDW state at low temperature. The neutron data indicated also a very subtle structural distortion, which deserves further study.

REFERENCES

[1] Grüner G., *Density Waves in Solids* (Addison-Wesley Publ.) 1994.
[2] Straub Th., Finteis Th., Claessen R., Steiner P., Hufner S., Blaha P., Oglesby C. S. and Bucher E., *Phys. Rev. Lett.*, **82** (1999) 4504.
[3] Fawcett E., *Rev. Mod. Phys.*, **60** (1988) 209.
[4] Kamihara Y., Watanabe T., Hirano M. and Hosono H., *J. Am. Chem. Soc.*, **130** (2008) 3296.
[5] Lebégue S., *Phys. Rev. B*, **75** (2007) 035110.
[6] Singh D. J. and Du M. H., arXiv:0803.0429 (2008).
[7] Xu Gang, Ming Wenmei, Yao Yugui, Dai Xi, Zhang Shou-Cheng and Fang Zhong, *Europhys. Lett.*, **82** (2008) 67002.
[8] Haule K., Shim J. H. and Kotliar G., arXiv:0803.1279 (2008).
[9] Mazin I. I., Singh D. J., Johannes M. D. and Du M. H., arXiv:0803.2740 (2008).
[10] Li Z., Chen G. F., Dong J., Li G., Hu W. Z., Zhou J., Wu D., Su S. K., Zheng P., Wang N. L. and Luo J. L., arXiv:0803.2572 (2008).
[11] Chen G. F., Li Z., Li G., Zhou J., Wu D., Dong J., Hu W. Z., Zheng P., Chen Z. J., Luo J. L. and Wang N. L., arXiv:0803.0128 (2008).
[12] Fradkin E., Kivelson S. and Oganesyan V., *Science*, **315** (2007) 196.